

A Novel MOEMS device: Detection of MEMS movements using free-standing Si_3N_4 suspended optical waveguides.

G. Altena, M. Dijkstra, G. van Elzaker, G. Venhorst, H.J.W.M. Hoekstra and P.V. Lambeck

Integrated Optical MicroSystems (formerly LDG), MESA⁺ Research Institute, University of Twente, P.O. Box 217, 7500 AE, Enschede, The Netherlands. E-Mail: g.altena@ewi.utwente.nl

We report on 100 nm thick free standing Silicon-nitride waveguide suspended in air used to detect MEMS movement by applying evanescent field sensing. We discuss both design and technological aspects for fabricating these devices as well as experimental results on the insertion loss of realised devices.

1 Introduction

In many MEMS structures it is required to monitor some characteristics of movements of subparts of the system. This might be during production in order to detect failures in an early stage or during operation. Detecting these characteristics during operation may be the primary function of the MEMS e.g. registration of the resonance frequency of cantilever sensors, or can be used for monitoring the condition of the system during its life cycle. Here optical methods show the advantage of contact less measurement of the required quantities. Using free space beams, interferometric methods enable to measure the spatial distribution of the deflections and resonance frequencies with large accuracy[1]. However probing the moving part with free space beams requires accessibility of that beam to the moving part, and together with the high cost of these bulky measurement systems, this limits their application to the production stage or to research conditions. For probing these characteristics during in situ operation integrated optical devices are expected to offer good perspectives. This probing can be based on the phenomenon, that characteristic properties of a guided mode, which propagates through an integrated optical waveguide channel, are influenced by the penetration of bodies into their evanescent field [2]. Common integrated optical circuits enable the subsequent conversion of the changes of these modal properties into a change of output power. These integrated optical read out systems enable the detection of resonance frequencies and of a weighted average value of the deflection of the moving part. In common integrated optical waveguides the decay length of these exponentially decaying evanescent fields is in the range 0.2- 1 micrometre, requiring a very intimate contact of the MEMS and the optical read out head. Here we propose a waveguiding structure showing decay lengths up to ten micrometer (section 2). These structures have been produced (section 3) and characterised (section 4). This type of structures, incorporated into an integrated optical read out system, such as a Mach-Zehnder interferometer (MZI)[3] is expected to be useful for probing moving parts, whether by a temporal contact (pressing an optical wafer to a MEMS wafer as a step during the production of the MEMS) or by being in a state of permanent contact (mechanical and optical chip are bonded together).

2 Simulation results

Common monomodal waveguiding structures consisting of a Si_3N_4 waveguiding core layer on top of a SiO_2 buffer layer are well suited for purely *refractive* detection where only the real part of the N_{eff} of the guided mode is affected by the movement of the MEMS body. However, in this case one is limited in both the detection range as the decay length of the exponentially decaying evanescent field is approximately $1\mu\text{m}$ and in the choice of the material of the MEMS as this is bounded by the fact that the refractive index of the material needs to be *below* the N_{eff} of the guided mode.

A Novel MOEMS device: Detection of MEMS movements using free-standing Si₃N₄ suspended optical waveguides.

Using the common waveguiding structure mentioned above the choice is small, SiO₂ or materials like MgO and teflons. The effects on the real part of the effective index ($\Delta N'_{\text{eff}}$) of driving a SiO₂ MEMS body into the evanescent field (distance to the upper surface of the waveguide is called 'airgap') of such common waveguide is illustrated by *dashed* line in Figure 1(a). Best interferometers[3] show a resolution in the order of magnitude of $\Delta N'_{\text{eff}} = 10^{-8}$ implying that range is limited to 2 μm .

It can be shown that the decay length of the evanescent field is proportional to

$$\frac{\lambda}{2\pi\sqrt{N_{\text{eff}}^2 - 1}} \text{ for TE polarisation} \quad (1)$$

$$\frac{n_{\text{core}}^2}{n_{\text{air}}^2} \frac{\lambda}{2\pi\sqrt{N_{\text{eff}}^2 - 1}} \text{ for TM polarisation} \quad (2)$$

From these equations can be seen that in order to increase the decay length TM polarised light of a large wavelength needs to be chosen while simultaneously the refractive index of the core layer should be much larger than 1 ($n_{\text{core}} \gg 1$ and the N_{eff} of the guided mode needs to be close to 1. A wavelength of 1550 nm is chosen as stable lasers of this wavelength are easily commercially available. The other conditions can be fulfilled using a *thin* (~ 100 nm) Si₃N₄ core layer with a refractive index $n = 2.0$ surrounded by air.

The purely refractive case however no longer holds for these thin freestanding Si₃N₄ waveguides as in this structures the guided modes in the waveguide become *leaky* because now the refractive index of the MEMS body is greater than N'_{eff} . Hence, in addition to N'_{eff} also the imaginary part of the N_{eff} , N''_{eff} , will be affected.

To calculate these effects on the propagating mode a *leaky mode* model was used, derived by Hoekstra *et al*[4]. Using this model the $\Delta N'_{\text{eff}}$ and $\Delta N''_{\text{eff}}$ have been calculated for several types of penetrating materials: Si, SiO₂ and Al, the latter being a commonly used electrode material, all with a thickness of 100 nm of the Si₃N₄ core. For convenience, $\Delta N''_{\text{eff}}$ is presented as modal attenuation (in dB/mm). Both are shown in Figure 1. All MEMS bodies are assumed to have semi-infinite thicknesses.

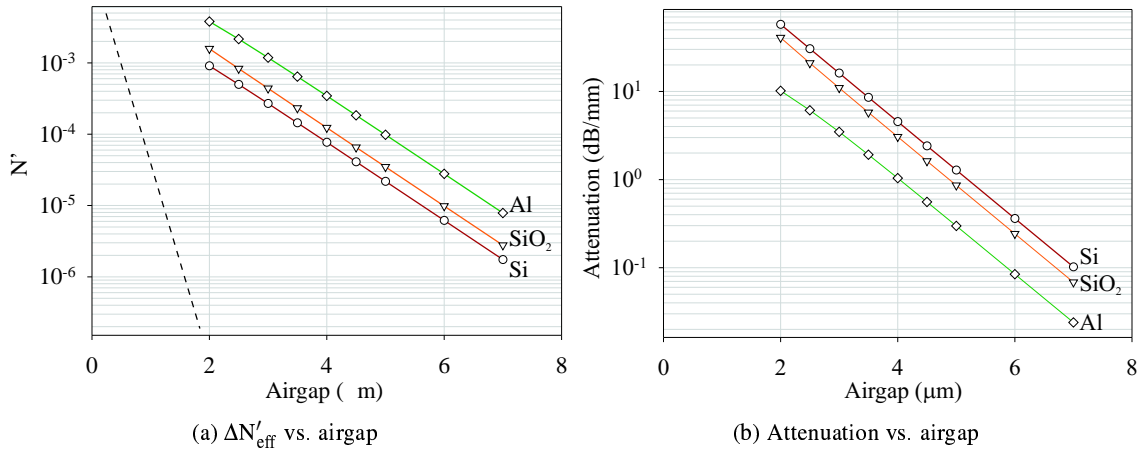


Figure 1: Change of the real part of the effective index, $\Delta N'_{\text{eff}}$ and attenuation versus the airgap for common waveguides (dashed, line, core thickness 300 nm, SiO₂ MEMS body) and free standing Si₃N₄ waveguiding structures (solid lines, core thickness 100 nm, Si, SiO₂ and Al MEMS bodies.), $\lambda = 1550$ nm, TM polarisation.

Figure 1 shows that for refractive measurements a Si₃N₄ membrane with an aluminium (Al) MEMS body is the most effective combination. $\Delta N'_{\text{eff}}$ effects are largest while at the same time

modal attenuation is lowest. An MZI[3] can cope well with asymmetries of about 10 dB. For a 4 mm interaction length this limits the detection range to airgap values in between approximately 3 μm to 10 μm . Note that also purely attenuation measurements are feasible.

3 Fabrication

The Si_3N_4 membranes and the common $\text{SiO}_2\text{Si}_3\text{N}_4\text{SiO}_2$ waveguiding structures are fabricated using standard deposition, lithography and etching techniques[3]. For realisation of the *adiabatic* taper structures needed for a loss free transition from the common waveguide structure (Si_3N_4 thickness 300 nm) to the freestanding waveguide (Si_3N_4 thickness 100 nm) some additional steps been developed. Of particular importance will be the effects of material stresses both in the membrane section and tapered sections. Schematic cross-sections of some of the needed structures are depicted the at bottom and side of Figure 3.

4 Characterisation

Several types of membrane structures have been fabricated. In Figure 2 a membrane (labelled 'A') is shown that is all-sided clamped via tapered sections ('B') on the common waveguide structure ('C'). The Si_3N_4 waveguiding core is thinned from 300 nm to 100 nm. In Figure 3 a Si_3N_4 core beam of 100 nm thick and 450 μm wide has been realised; here the membrane beam is supported by 50 μm wide Si beams to strengthen the structure. Note that empty regions aside the membrane waveguide enable readout of rotating mirrors.

Both structures show smooth surfaces without any *curtaining*. Tensile stresses are sufficiently low to avoid also any cracking. A yield over 90% can easily be obtained.

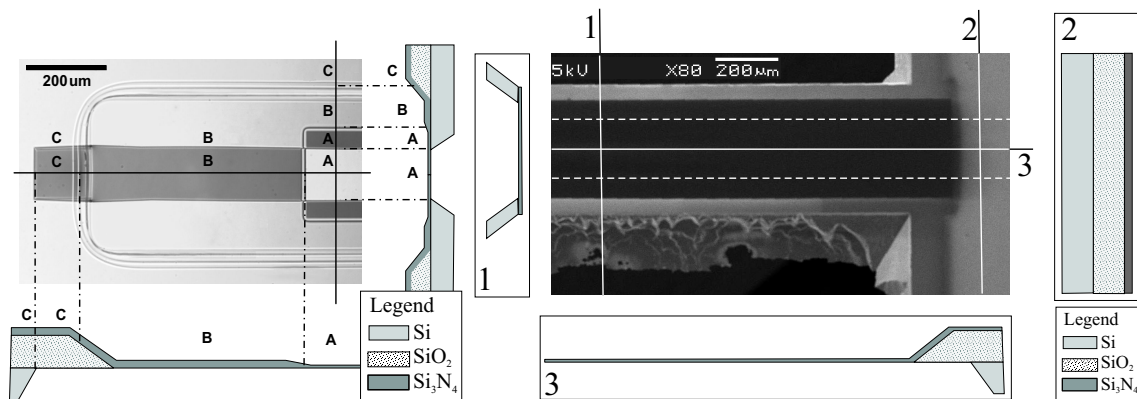


Figure 2: Micrograph of a 100 nm thick Si_3N_4 membrane (top view). Cross-sections along the two solid lines are presented.

Figure 3: SEM picture of a realised Si_3N_4 membrane on a Si bridge. The two Si beams that act as supports for the Si_3N_4 membrane are 50 μm wide. Cross-sections are along the three solid lines labelled 1 through 3. The intended location of the waveguides are indicated by the dashed line.

Insertion loss measurements were carried out on straight ridge-type channel waveguides. Half of them have been implemented into the structures as given Figure 2 while the other half was realised in the common structure. The membrane section is 5 mm long, 3 mm wide and 100 nm thick. The (single-mode) waveguide channels have widths of 6 μm and a ridge height of 6. Light was coupled into and out of the waveguides using fibre-to-chip coupling. Results for a wavelength of 1550 nm for both TE and TM polarisation are given in Table 1.

Table 1: Insertion loss (and standard deviation σ) of chips containing 3 cm long straight waveguides of various type, $\lambda = 1550$ nm.

	TE average (dB)	σ (dB)	TM average (dB)	σ (dB)
Common waveguide only	-18.3450	0.1202	-16.6161	0.8559
Common waveguide with a membrane	-20.9200	0.5374	-24.4373	1.4320

From the data given in Table 1 the additional attenuation induced by the tapering and membrane formation can be calculated to be 2.6 dB for TE polarisation and 7.8 dB for TM polarisation. This attenuation is mainly attributed to an increased scattering at the Si₃N₄-air interface (as a result of the thinning of the Si₃N₄ layer and the KOH etching) and in addition to some scattering at the tapered sections.

The difference of the effect of the surface scattering between the two polarisations can be estimated by performing Beam Propagation Methods (BPM) simulations on free standing waveguides with an artificially induced roughness. Preliminary BPM simulations show that the out-of-plane scattering is a large contributor to the difference in the attenuation in the Si₃N₄ membrane waveguide between TE and TM polarisation.

5 Conclusion

We have shown the feasibility of freestanding ultra-thin Si₃N₄ membrane as waveguides. Yields of larger than 90% have been achieved. Membrane induced losses are at a wavelength of 1550 nm approximately 7.8 dB for TM polarisation and 2.6 dB for TE polarisation. Calculations show that roughness induced surface scattering is the main cause of these losses. Roughness is expected to be reduced remarkably by some changes in the process flow.

6 Acknowledgements

This work is part of the OCMMM project funded by the European community under the "Competitive and Sustainable Growth" program.

References

- [1] P. Aswendt, C.D. Schmidt, D. Zielke, and S. Schubert. Inspection system for mems characterization on wafer level using espi. In *Proceedings of SPIE, Vol. 4400*, pages 43–50, 2001.
- [2] W.Lukosz. Integrated optical nanomechanical devices as modulators, switches and tunable wavelength filters and as acoustical sensors. In *Proceedings of SPIE, Vol. 1793*, pages 214–234, 1992.
- [3] R.G. Heideman and P.V. Lambeck. Remote opto-chemical sensing with extreme sensitivity: design, fabrication and performance of a pigtailed integrated optical phase-modulated Mach-Zehnder interferometer system. *Sensors and Actuators B*, 61:100–127, 1999.
- [4] H.J.W.M. Hoekstra, J.C. van't Spijker, and H.M.M. Klein Koerkamp. Ray picture for prism-film coupling. *Journal of the Optical Society of America A*, 10(10):2226–2230, 1993.